Electronic Supplementary Information

A Multifunctional Double Walled Zirconium Metal-Organic Framework: High Performance of CO_2 Adsorption and Separation, Detecting Explosives in Aqueous Phase

Xiaodong Sun,[a,c] Xu Li,[b] Shuo Yao,[a] Rajamani Krishna,[d] Jiaming Gu,[a] Guanghua Li,[a] Yunling Liu*[a]

[a] *State Key Laboratory of Inorganic Synthesis and Preparative Chemistry, College of Chemistry, Jilin University, Changchun 130012, P. R. China*
[b] *School of Chemical Engineering and Light Industry, Guangdong University of Technology, Guangzhou 510006, Guangdong, P. R. China.*
[c] *Institute of Clean Energy Chemistry, Key Laboratory for Green Synthesis and Preparative Chemistry of Advanved Materials, College of Chemistry, Liaoning University, Shenyang 110036, China*
[d] *Van't Hoff Institute For Molecular Sciences, University of Amsterdam, Science Park 904, 1098 XH Amsterdam, The Netherlands*

Table of contents

1. XRD and TGA characterization of JLU-Liu45

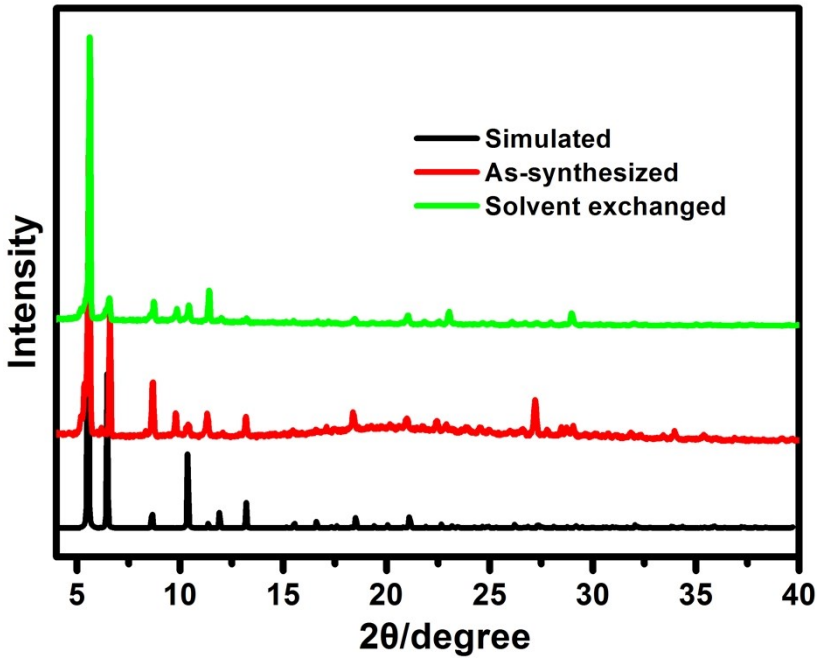

Fig. S1 PXRD patterns of **JLU-Liu45** for simulated, as-synthesized and CH_3CN solvent exchanged sample.

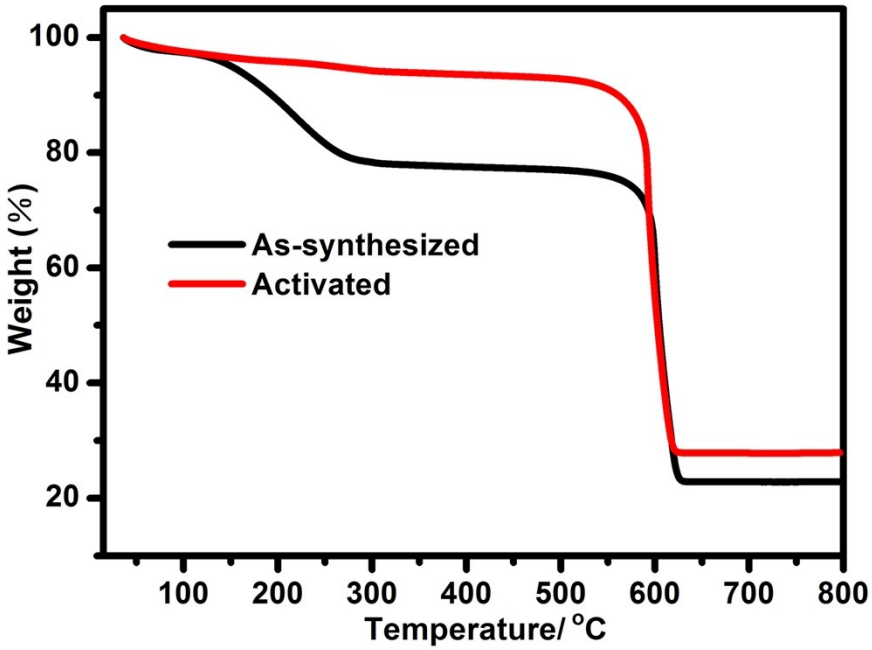

Fig. S2 TGA curves of **JLU-Liu45** for the as-synthesized and activated sample.

2. Structure description of JLU-Liu45

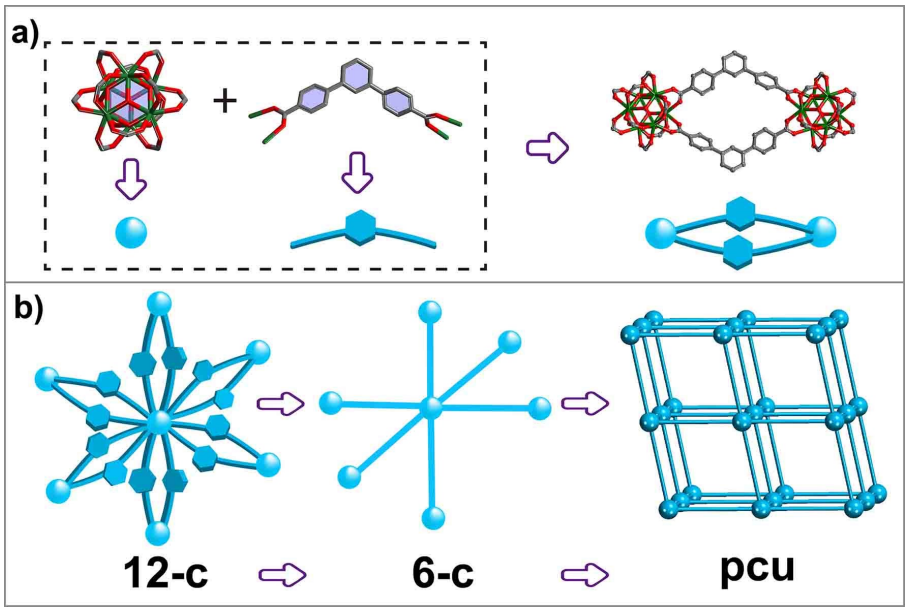

Fig. S3 Double walled building blocks assembled by two $Zr_6O_4(OH)_4(CO_2)_{12}$ SBUs and two C2-symmetric V-shaped H_2DCPB ligands (a); the 12-c building blocks with double wall can be simplified to a 6-c node and form the 6-c network with pcu topology (b). (Color scheme: carbon = grey; oxygen = red; zirconium = dark green).

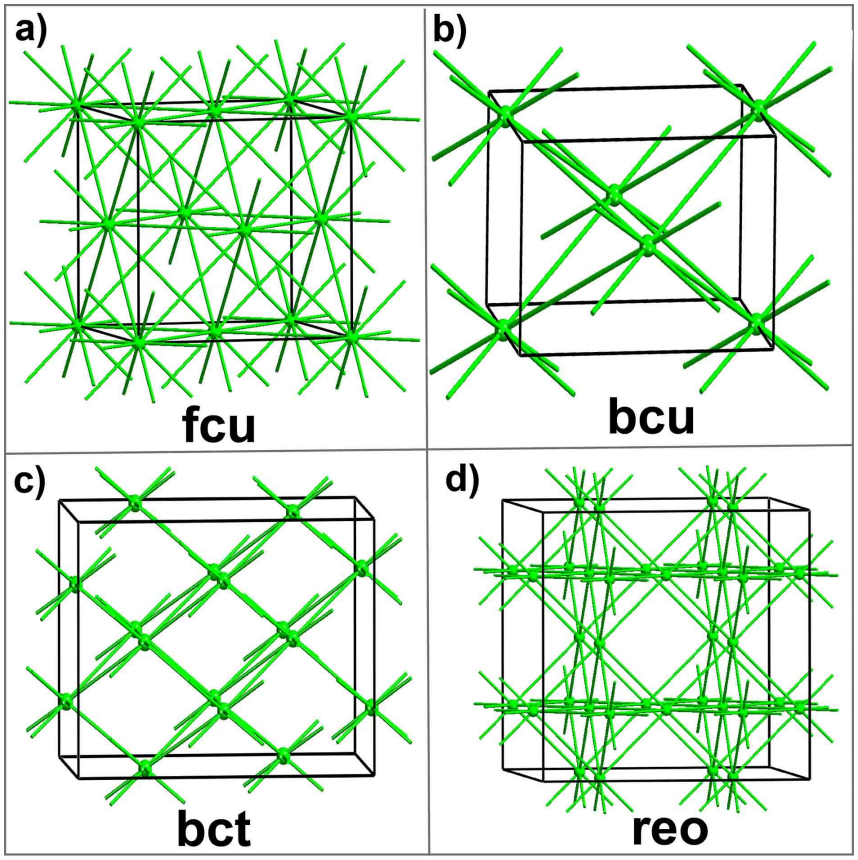

Fig. S4 Representative network topologies in reported Zr-MOFs constructed by dicarboxylate ligands.

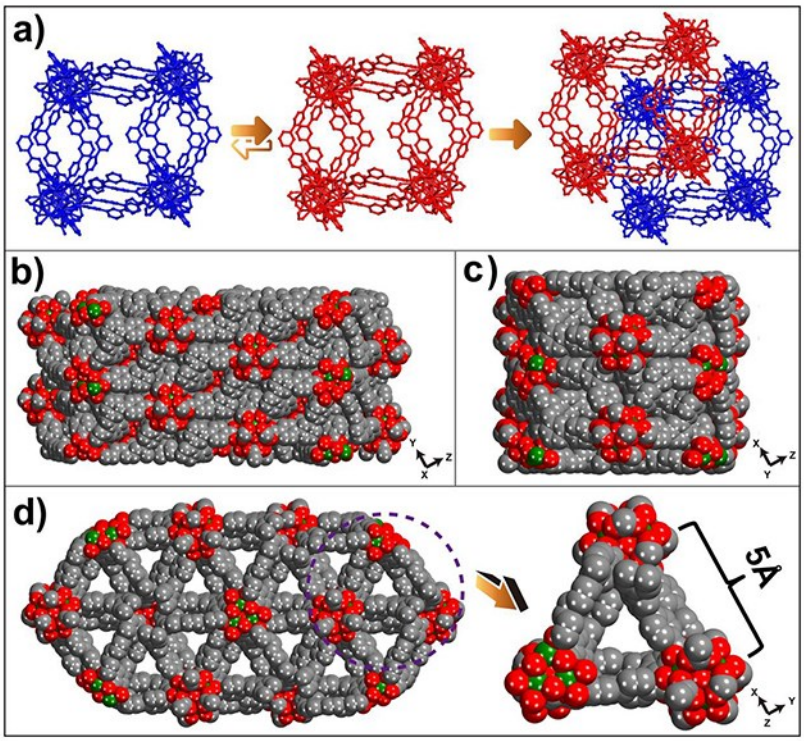

Fig. S5 (a) The formation of 3D interpenetrated framework; (b), (c) and (d) space-filling representations of the structure of **JLU-Liu45** viewed along the [100], [010] and [001] directions, respectively, and the dimension of triangle windows about 5 Å considering the van der Waals radius.

3. Stability test of JLU-Liu45

The thermal and chemical stability of **JLU-Liu45** was examined. The thermal stability was assessed by thermo gravimetric analysis (TGA) under an atmospheric environment. The high decomposition temperature which can reach up to 550 ^{o}C reveals the notable thermal stability of the **JLU-Liu45** material. On the other hand, to estimate the chemical stability of the framework, the as-synthesized **JLU-Liu45** samples were immersed in HCl and NaOH aqueous solutions with a pH range from 0 to 11, and different organic solutions at room temperature for 48 h. The PXRD patterns were completely maintained from the harsh chemical environment. Although slight differences of the peak strength can be observed, the N_2 adsorption measurement of the samples after stability test demonstrated that **JLU-Liu45** exhibited excellent chemical stability. PXRD patterns for **JLU-Liu45** sample before and after measuring the water adsorption isotherm also indicate its water stability. Because of the following reasons, **JLU-Liu45** exhibits commendable stability: (1) Zr^{4+} has high charge density, polarizes the O atoms of the carboxylate groups to form strong Zr-O bonds with significant covalent character. (2) Double walled framework can improve the stability of the material. (3) Interpenetration framework can minimize the empty space and further enhance the stability of the material. In conclusion, **JLU-Liu45** is highly robust and deserves further exploring in practical applications.

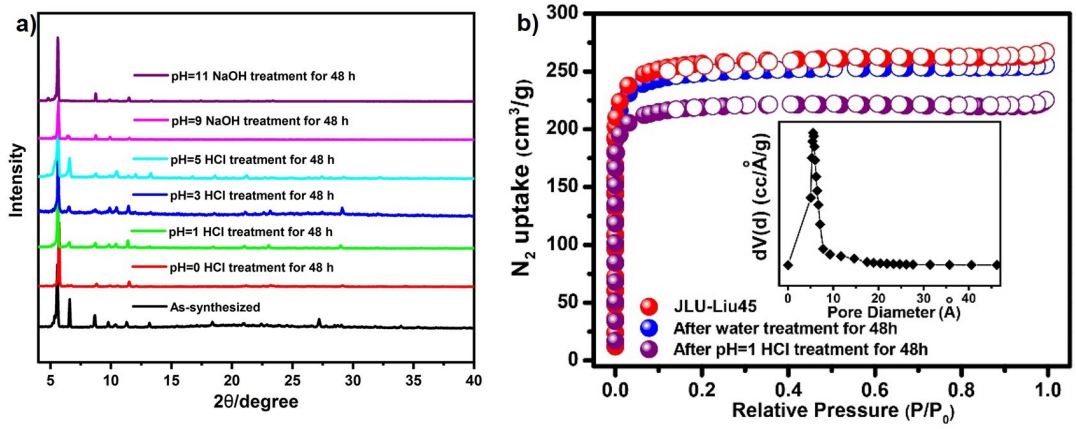

Fig. S6 (a) PXRD patterns and (b) N_2 isotherms of **JLU-Liu45** after immersed in aqueous solutions with different pH values at room temperature for 48 h and the corresponding pore size distribution curve calculated using DFT method (insert).

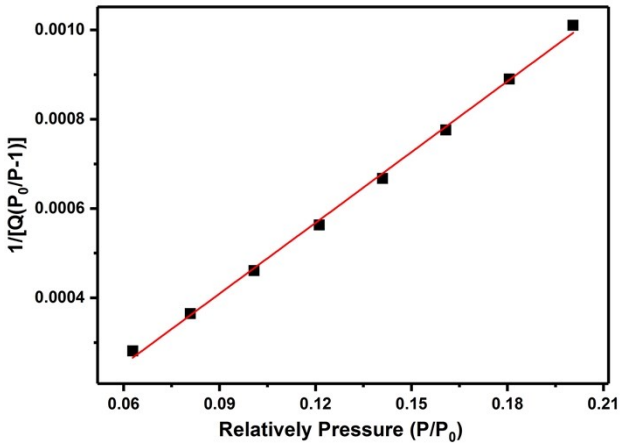

Fig. S7 The linear fitting curve for calculating BET surface areas of **JLU-Liu45**.

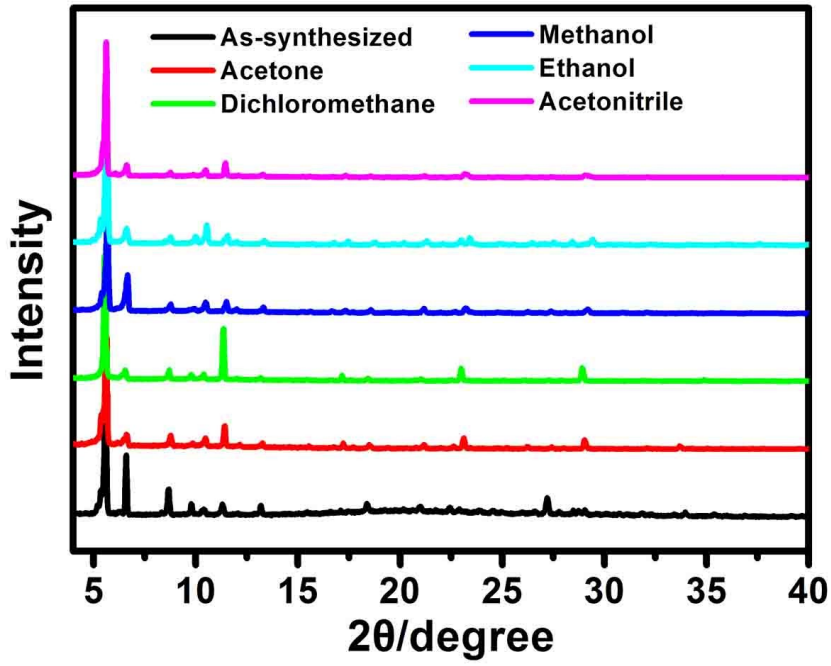

Fig. S8 PXRD patterns of **JLU-Liu45** for as-synthesized and the sample immersed in different organic solutions at room temperature for 48 h.

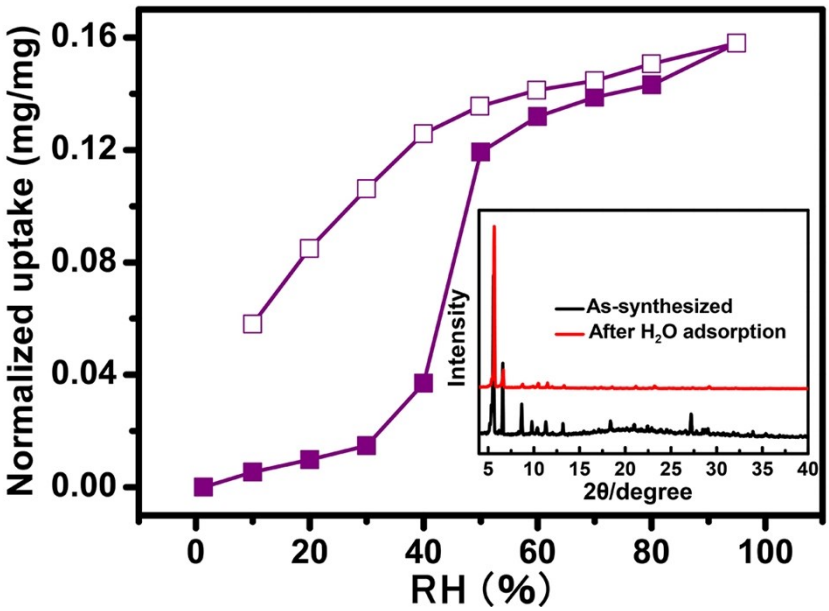

Fig. S9 Water adsorption isotherm of **JLU-Liu45** (experimental condition: T = 298 K, P = 1 bar; N_2 carrier gas). PXRD patterns (insert graph) for **JLU-Liu45** sample before and after measuring the water adsorption isotherm.

4. Gas adsorption and separation studies

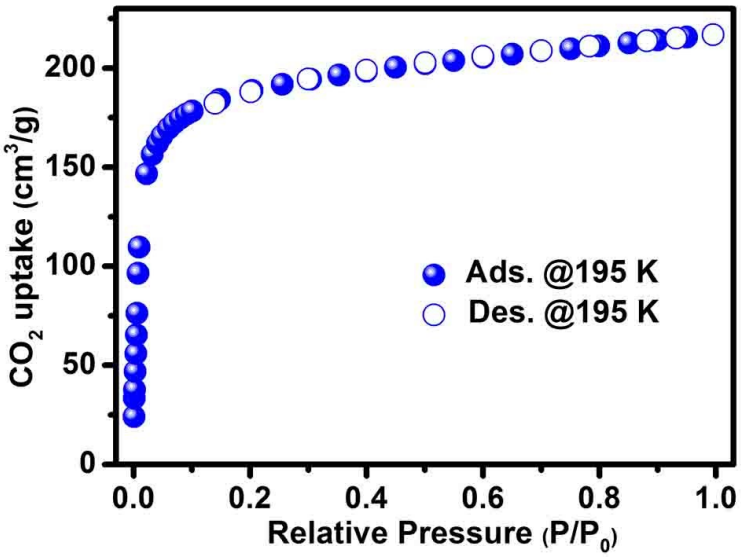

Fig. S10 The CO_2 adsorption isotherm for **JLU-Liu45** at 195 K under 1 bar.

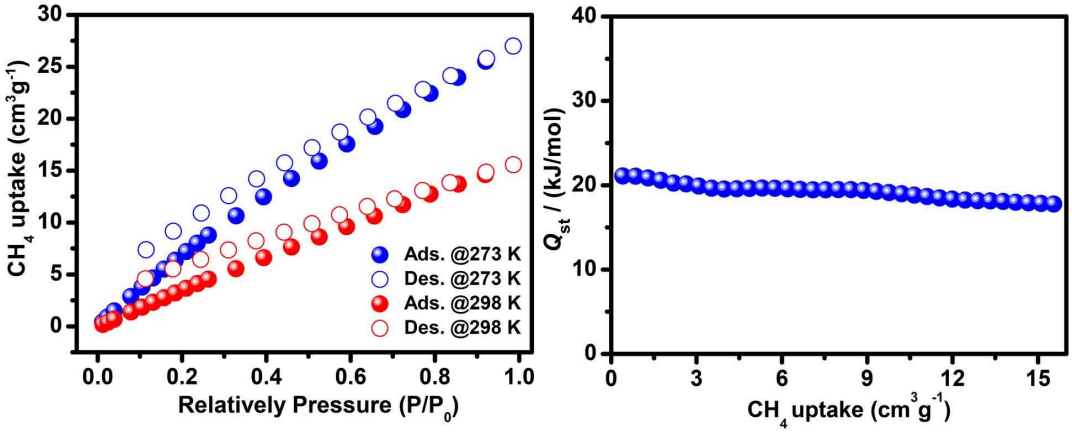

Fig. S11 The CH_4 isotherms for **JLU-Liu45** at 273 and 298 K under 1 bar and Q_{st} of CH_4 for **JLU-Liu45**.

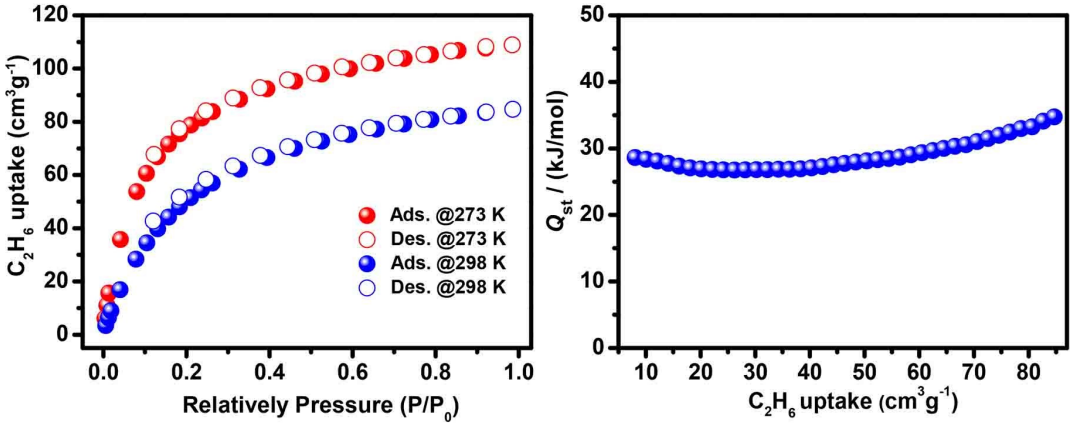

Fig. S12 The C_2H_6 isotherms for **JLU-Liu45** at 273 and 298 K under 1 bar and Q_{st} of C_2H_6 for **JLU-Liu45**.

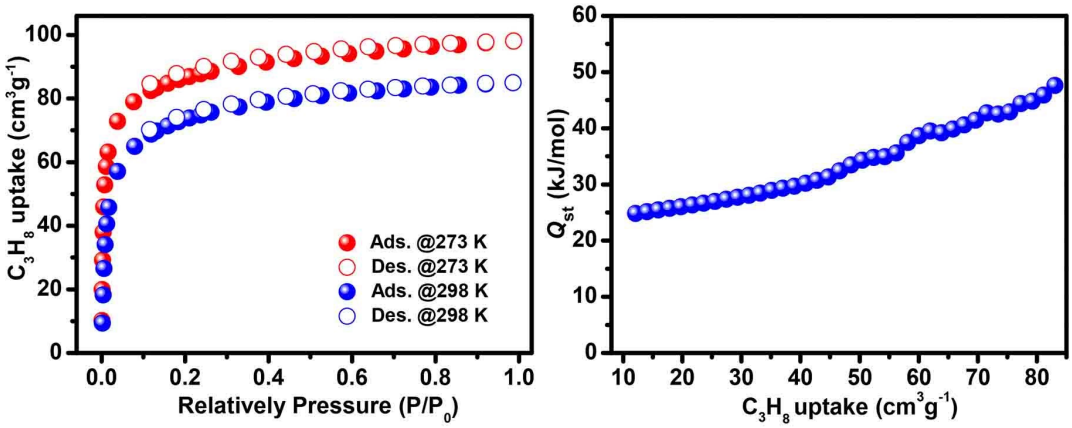

Fig. S13 The C_3H_8 isotherms for **JLU-Liu45** at 273 and 298 K under 1 bar and Q_{st} of C_3H_8 for **JLU-Liu45**.

5. Calculation procedures of selectivity from IAST

The measured experimental data is excess loadings (q^{ex}) of the pure components N_2, CO_2, CH_4, C_2H_6 and C_3H_8 for **JLU-Liu45**, which should be converted to absolute loadings (q) firstly.

$$q = q^{ex} + \frac{pV_{pore}}{ZRT}$$

Here Z is the compressibility factor. The Peng-Robinson equation was used to estimate the value of compressibility factor to obtain the absolute loading, while the measure pore volume 0.38 $cm^3\ g^{-1}$ is also necessary.

The dual-site Langmuir-Freundlich equation is used for fitting the isotherm data at 298 K.

$$q = q_{m_1} \times \frac{b_1 \times p^{1/n_1}}{1 + b_1 \times p^{1/n_1}} + q_{m_2} \times \frac{b_2 \times p^{1/n_2}}{1 + b_2 \times p^{1/n_2}}$$

Here p is the pressure of the bulk gas at equilibrium with the adsorbed phase (kPa), q is the adsorbed amount per mass of adsorbent (mol kg^{-1}), q_{m1} and q_{m2} are the saturation capacities of sites 1 and 2 (mol kg-1), b_1 and b_2 are the affinity coefficients of sites 1 and 2 (1/kPa), n_1 and n_2 are the deviations from an ideal homogeneous surface.

The selectivity of preferential adsorption of component 1 over component 2 in a mixture containing 1 and 2, perhaps in the presence of other components too, can be formally defined as

$$S = \frac{q_1/q_2}{p_1/p_2}$$

q_1 and q_2 are the absolute component loadings of the adsorbed phase in the mixture. These component loadings are also termed the uptake capacities. We calculate the values of q_1 and q_2 using the Ideal Adsorbed Solution Theory (IAST) of Myers and Prausnitz.

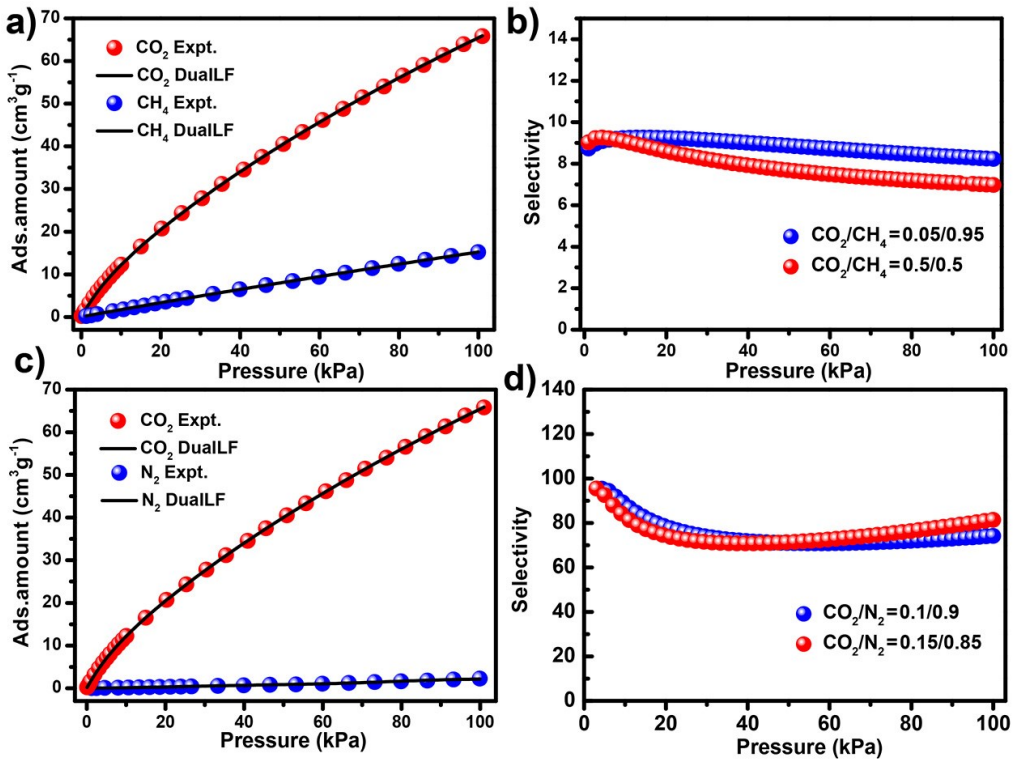

Fig. S14 CO_2, CH_4 and N_2 adsorption isotherms at 298 K along with the dual-site Langmuir Freundlich (DSLF) fits (a and c); gas mixture adsorption selectivity are predicted by IAST at 298 K and 100 kPa for **JLU-Liu45** (b and d).

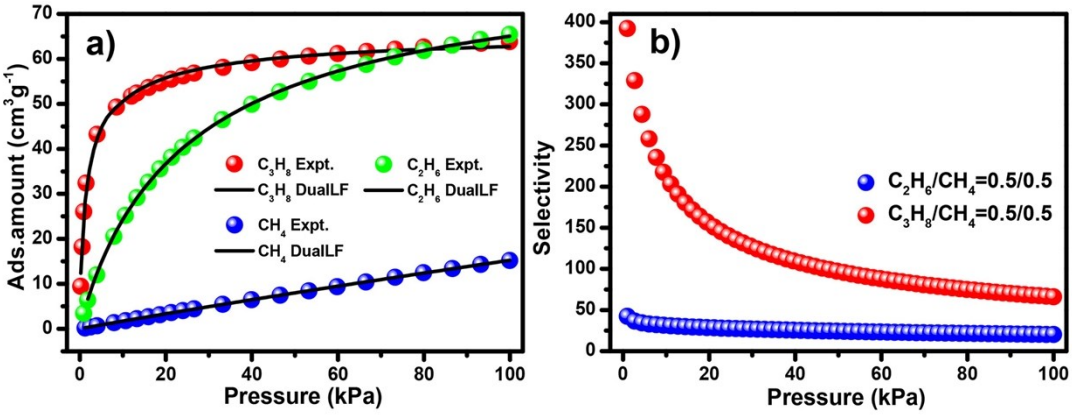

Fig. S15 CH_4, C_2H_6 and C_3H_8 adsorption isotherms at 298 K along with the dual-site Langmuir Freundlich (DSLF) fits (a); gas mixture adsorption selectivity are predicted by IAST at 298 K and 100 kPa for **JLU-Liu45** (b).

6. Transient breakthrough of mixtures in fixed bed adsorbers

The performance of industrial fixed bed adsorbers is dictated by a combination of adsorption selectivity and uptake capacity. For a proper evaluation of the separation performance, we performed transient breakthrough simulations using the simulation methodology described in the literature. For the breakthrough simulations, the following parameter values were used: length of packed bed, L = 0.3 m; voidage of packed bed, ε = 0.4; superficial gas velocity at inlet, u = 0.04 m/s. The transient breakthrough simulation results are presented in terms of a *dimensionless* time, τ, defined by dividing the actual time, t, by the characteristic time, $\frac{L\varepsilon}{u}$.

Notation

c_i	molar concentration of species i in gas mixture at exit of adsorber, mol m^{-3}
c_{i0}	molar concentration of species i in gas mixture at inlet of adsorber, mol m^{-3}
L	length of packed bed adsorber, m
t	time, s
u	superficial gas velocity in packed bed, m s^{-1}

Greek letters

τ	time, dimensionless

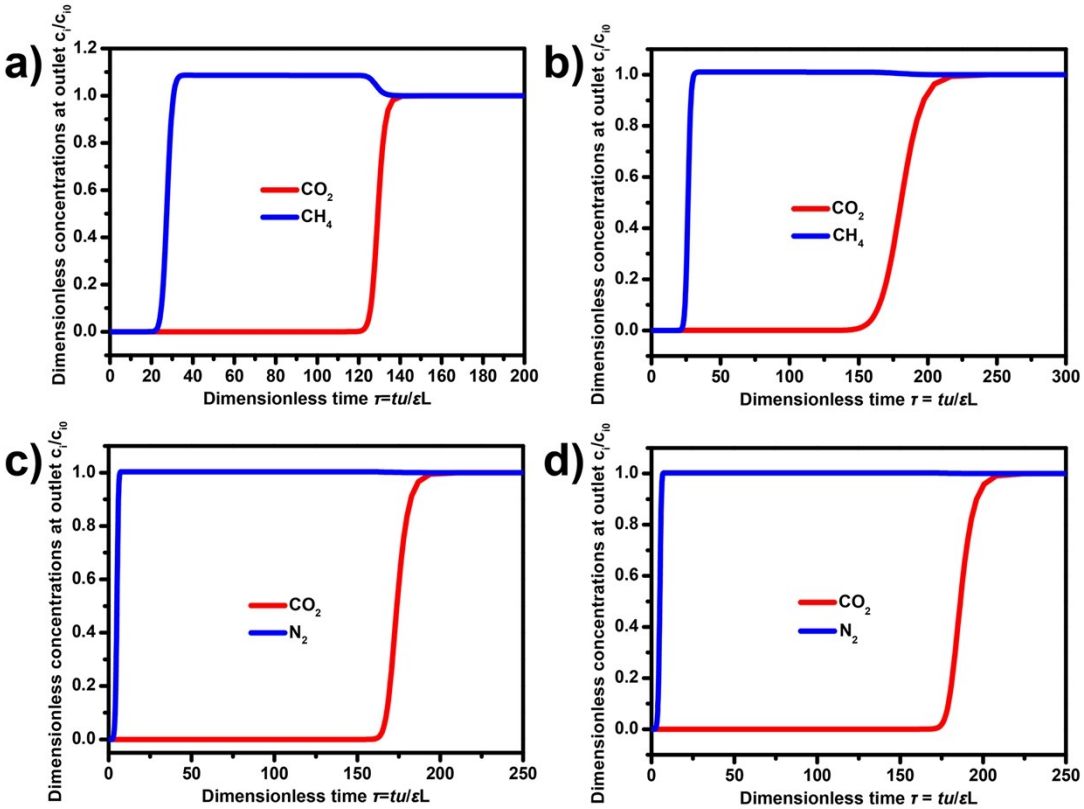

Fig. S16 Transient breakthrough simulations for separation of 50/50 and 5/95 (a and b) CO_2/CH_4, 15/85 and 10/90 (c and d) CO_2/N_2 mixtures containing. The total inlet pressure is 100 kPa. The y-axis is the dimensionless concentrations at the exit, normalized with respect to the inlet concentrations.

7. Computational simulation studies of CO_2 adsorption

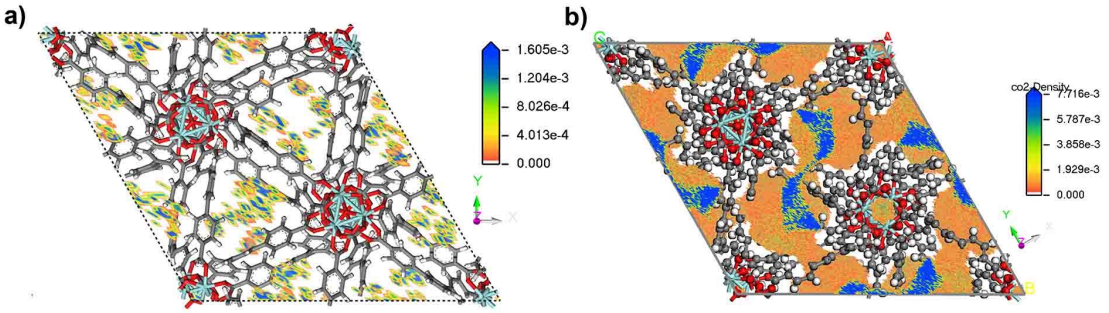

Fig. S17 Density distribution of the center-of-mass of CO_2 molecules in one unit cell of **JLU-Liu45** framework at 298 K and 1 bar simulated by GCMC method (a and b).

8. Detection of selected nitroaromatics

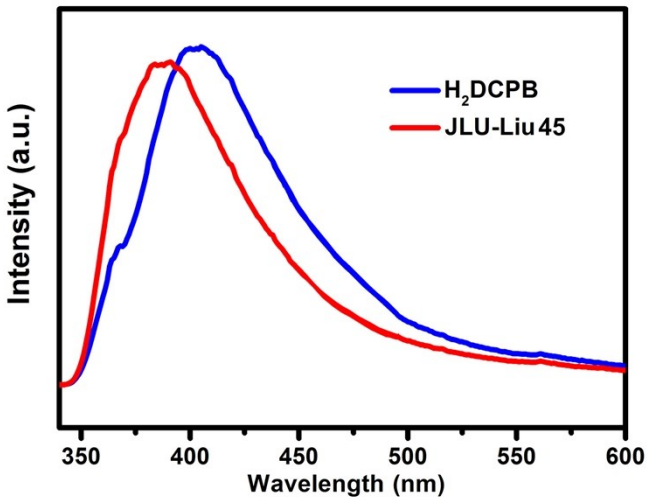

Fig. S18 Solid-state photoluminescent spectra of **JLU-Liu45** and free H_2DCPB ligand excited at 323 nm at room temperature.

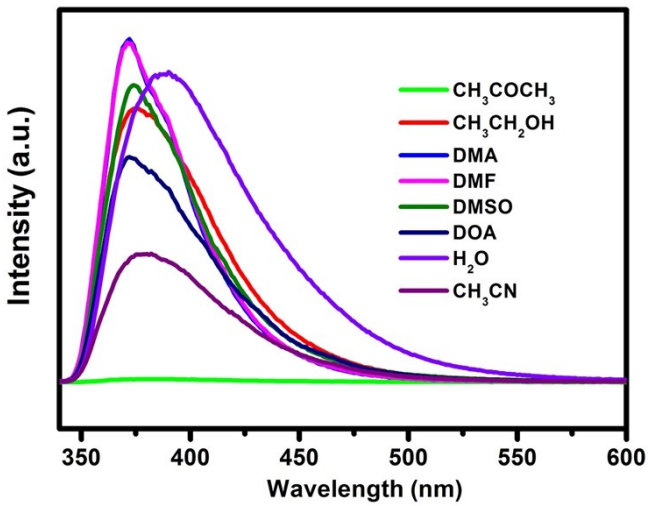

Fig. S19 Photoluminescent spectra of **JLU-Liu45** dispersed in different solvents excited at 323 nm.

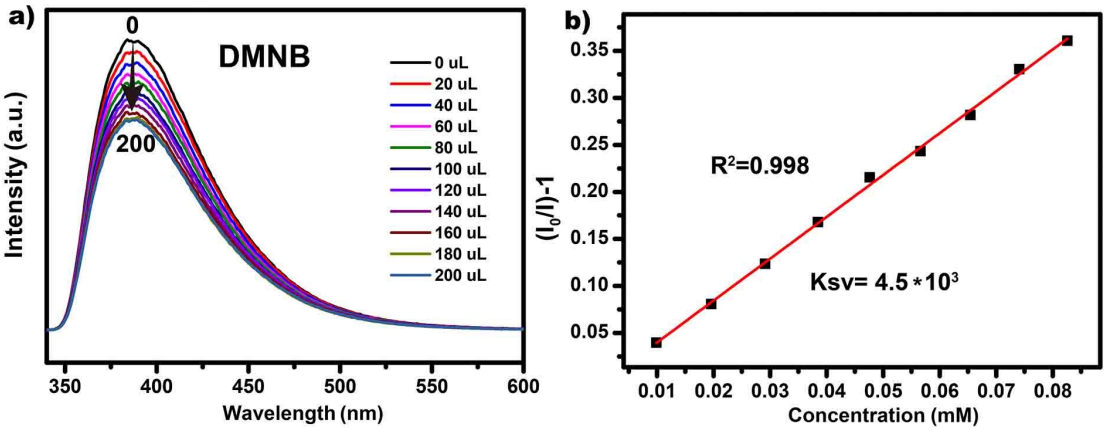

Fig. S20 a) Effect on the emission spectra of **JLU-Liu45** dispersed in water upon the incremental addition of 200 μL (1 mM, 20 μL addition each time) aqueous solution of DMNB. b) SV plot of DMNB.

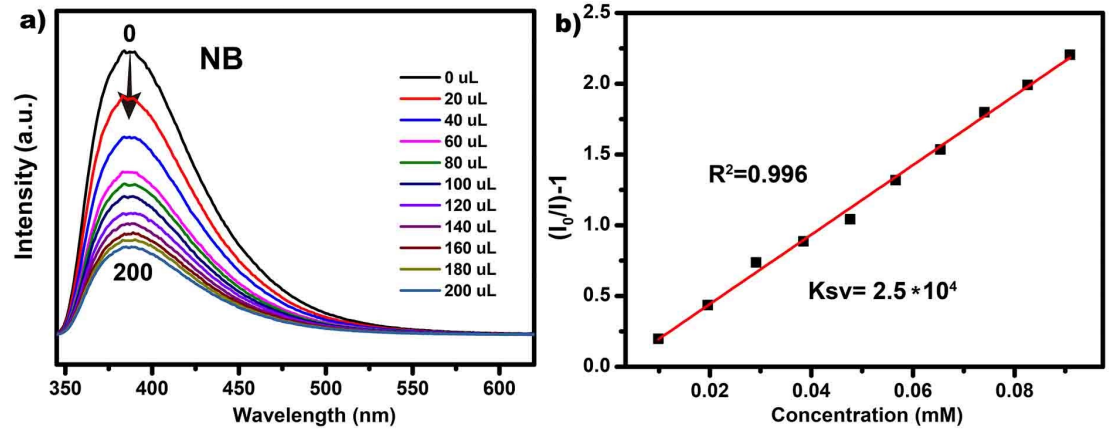

Fig. S21 a) Effect on the emission spectra of **JLU-Liu45** dispersed in water upon the incremental addition of 200 μL (1 mM, 20 μL addition each time) aqueous solution of NB. b) SV plot of NB.

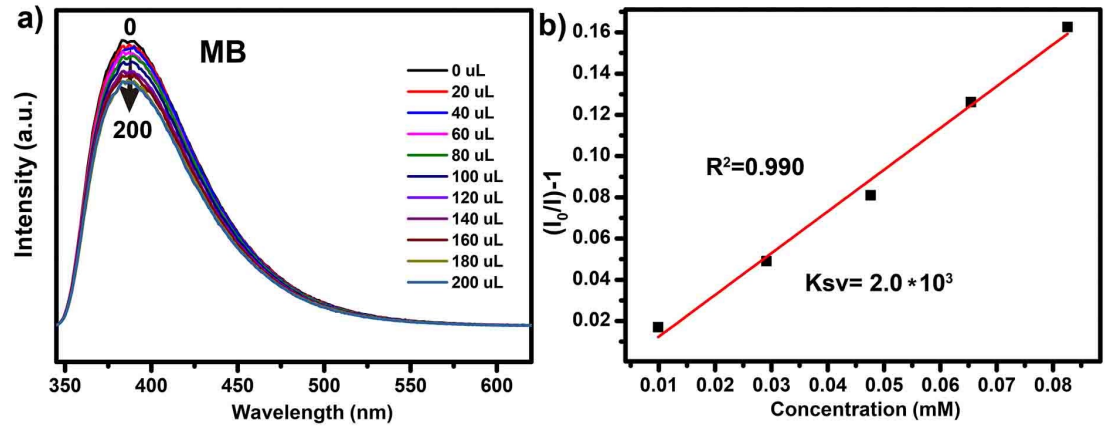

Fig. S22 a) Effect on the emission spectra of **JLU-Liu45** dispersed in water upon the incremental addition of 200 μL (1 mM, 20 μL addition each time) aqueous solution of MB. b) SV plot of MB.

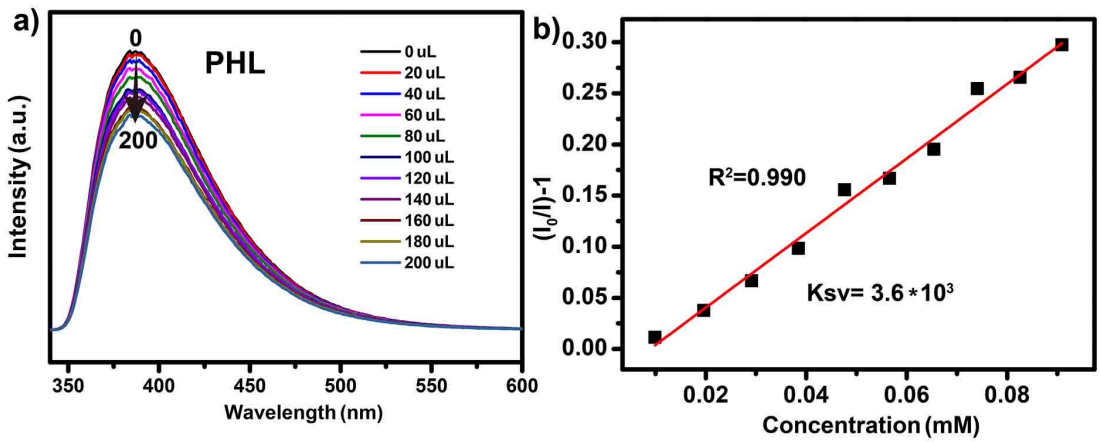

Fig. S23 a) Effect on the emission spectra of **JLU-Liu45** dispersed in water upon the incremental addition of 200 μL (1 mM, 20 μL addition each time) aqueous solution of PHL. b) SV plot of PHL.

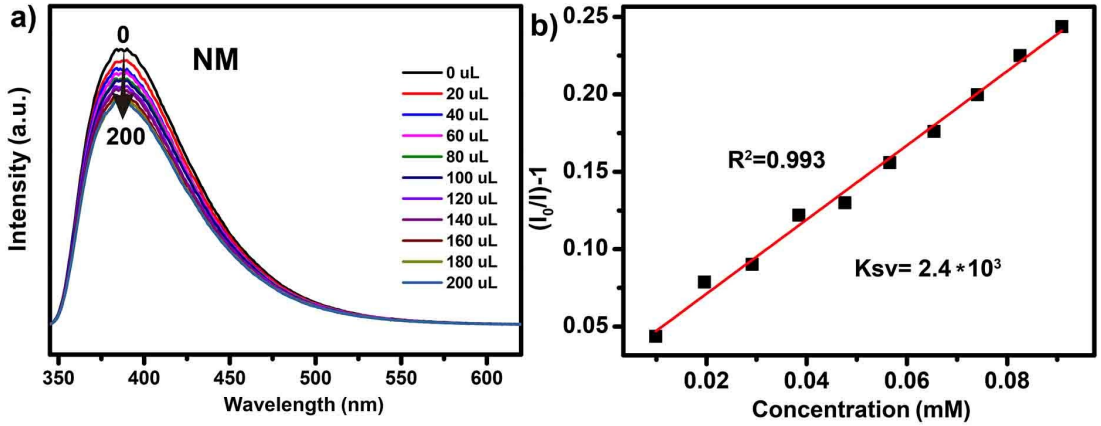

Fig. S24 a) Effect on the emission spectra of **JLU-Liu45** dispersed in water upon the incremental addition of 200 μL (1 mM, 20 μL addition each time) aqueous solution of NM. b) SV plot of NM.

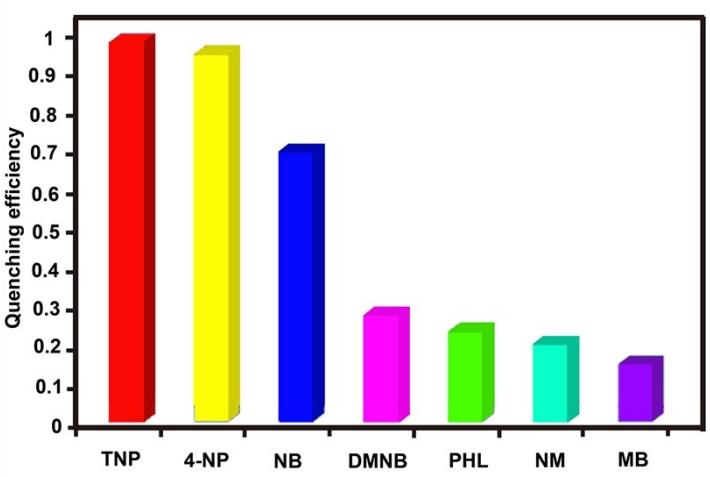

Fig. S25 The fluorescence quenching efficiency for different analytes.

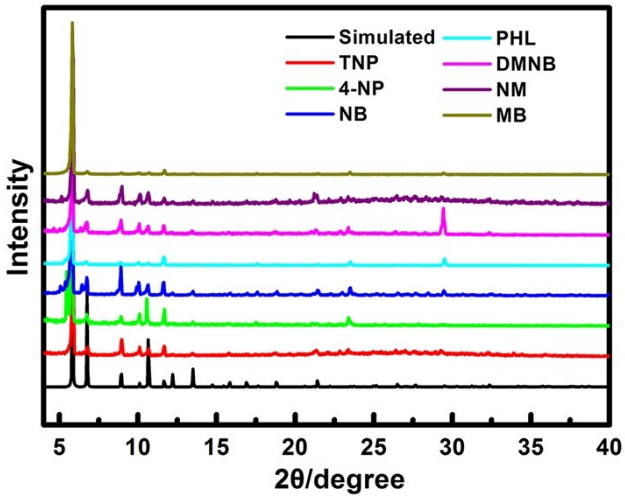

Fig. S26 Powder X-ray diffraction (PXRD) patterns of **JLU-Liu45** after the detection of antibiotics and nitroaromatics.

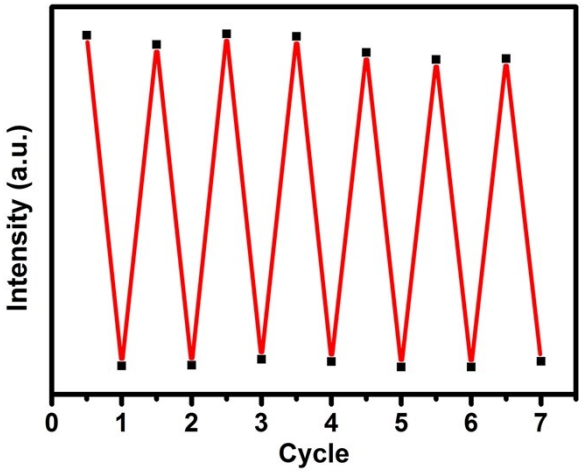

Fig. S27 Reproducibility of the quenching ability of **JLU-Liu45** dispersed in water in the presence of 1 mM aqueous solution of TNP.

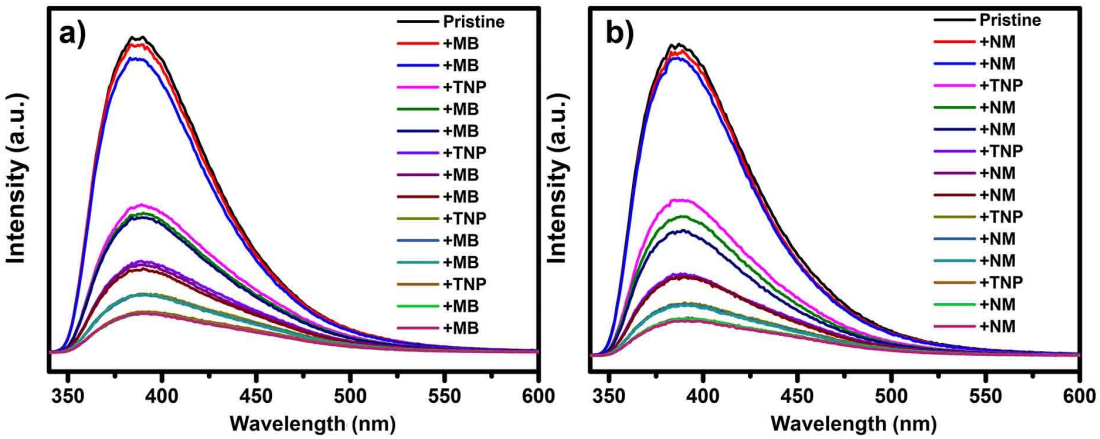

Fig. S28 Tracked emission spectra of **JLU-Liu45** upon the addition of 1 mM aqueous solution of a) MB b) NM followed by 1 mM aqueous solution of TNP, respectively (20 μL addition each time).

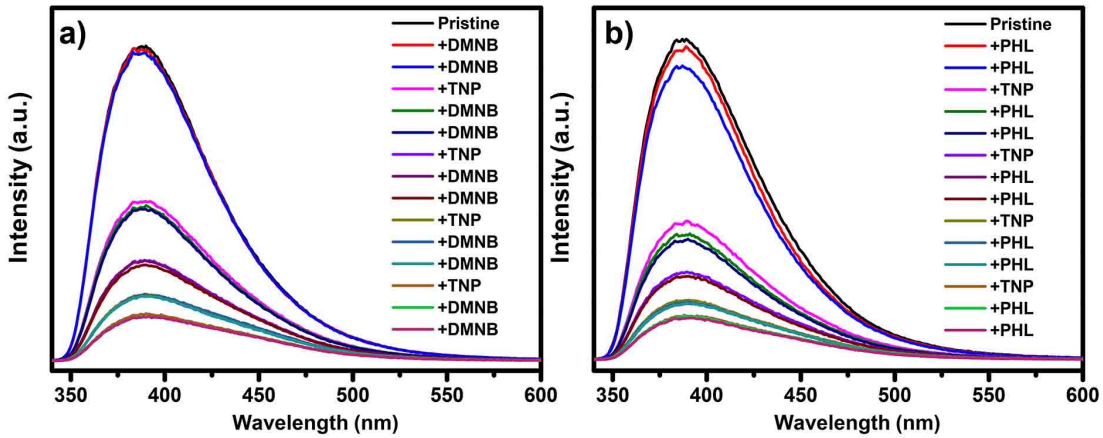

Fig. S29 Tracked emission spectra of **JLU-Liu45** upon the addition of 1 mM aqueous solution of a) DMNB b) PHL followed by 1 mM aqueous solution of TNP, respectively (20 μL addition each time).

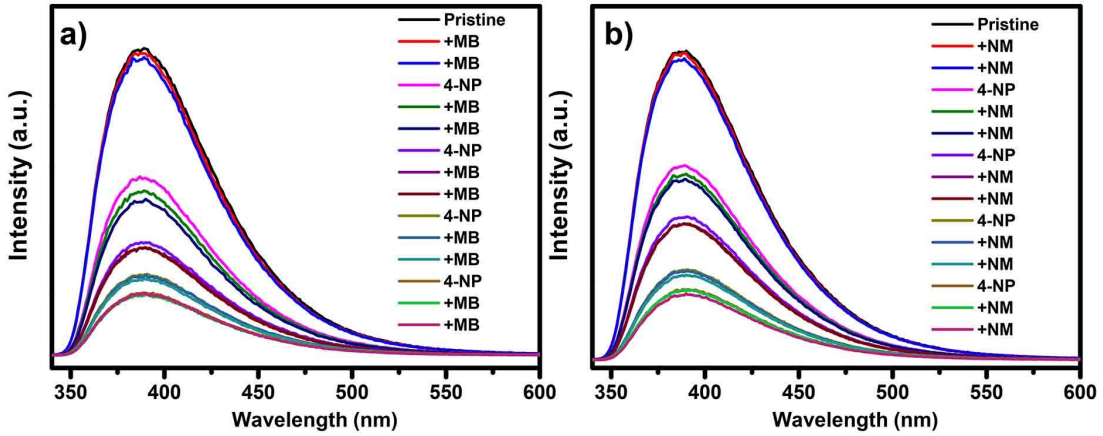

Fig. S30 Tracked emission spectra of **JLU-Liu45** upon the addition of 1 mM aqueous solution of a) MB b) NM followed by 1 mM aqueous solution of 4-NP, respectively (20 μL addition each time).

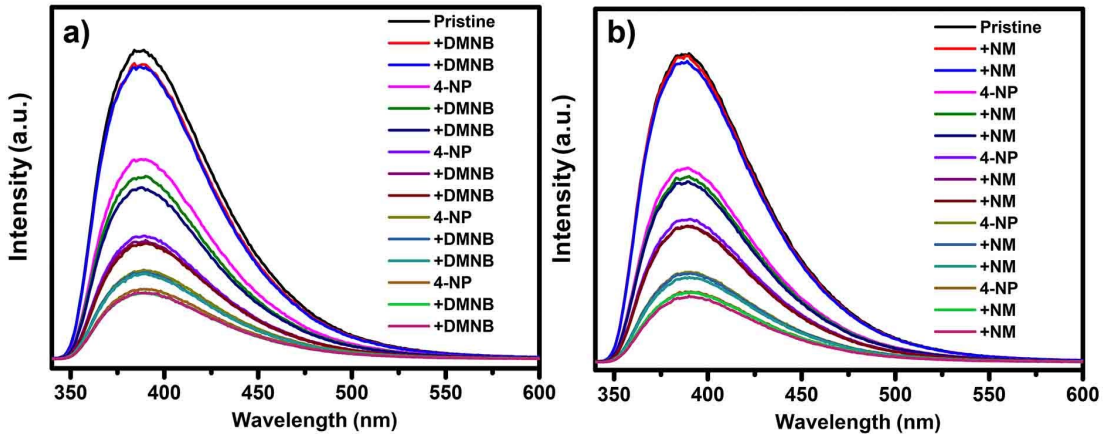

Fig. S31 Tracked emission spectra of **JLU-Liu45** upon the addition of 1 mM aqueous solution of a) DMNB b) PHL followed by 1 mM aqueous solution of 4-NP, respectively (20 μL addition each time).

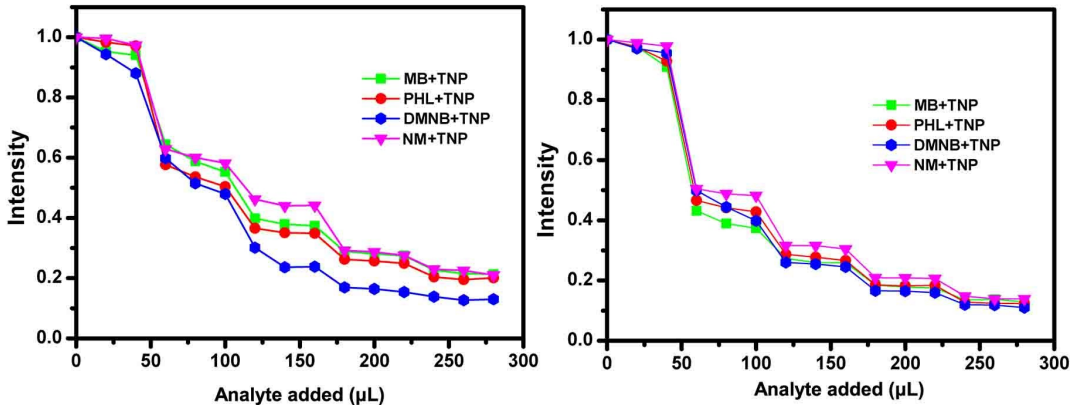

Fig. S32 The selective detection of 4-NP a) and TNP b) on **JLU-Liu45** in the presence of PHL, MB, NM or DMNB in water.

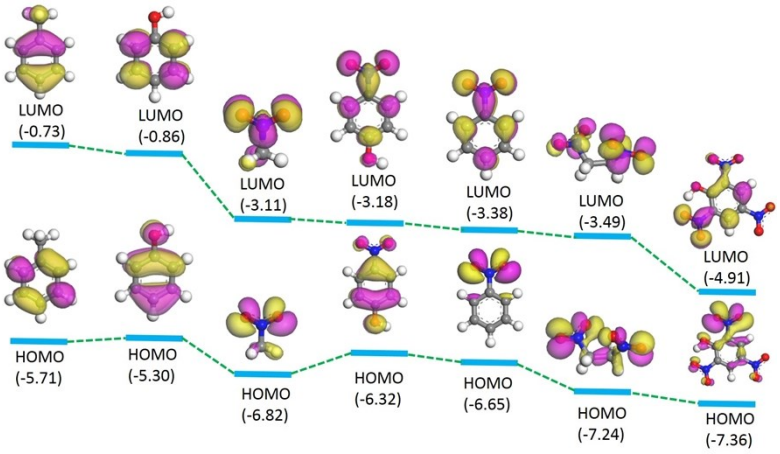

Fig. S33 DFT-calculated HOMO-LUMO energy profiles of MB, PHL, NM, 4-NP, NB, DMNB and TNP (from left to right).

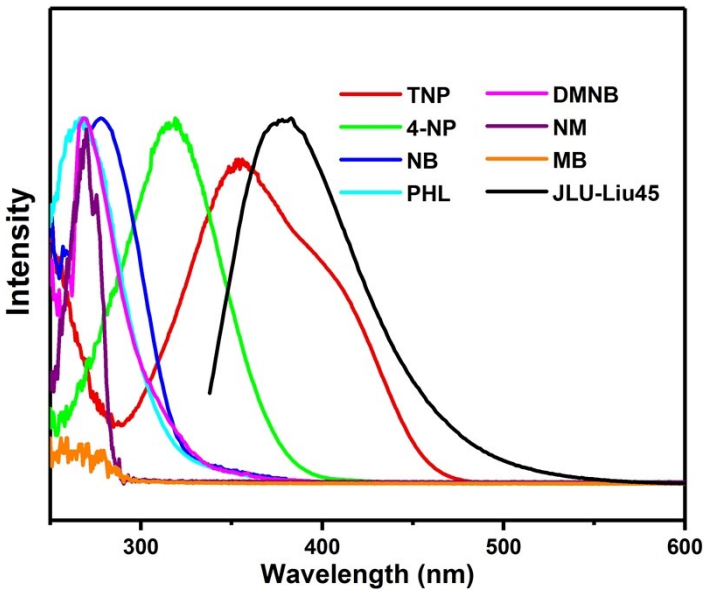

Fig. S34 Spectral overlap between normalized absorption spectra of selected organic explosives and the normalization emission spectrum of **JLU-Liu45**.

9. Tables

Table S1. Crystal data and structure refinement for **JLU-Liu45**

Compound	**JLU-Liu45**
formula	$C_{126}H_{92}N_2O_{35}Zr_6$
formula weight	2741.34
temp (K)	296(2) K
wavelength (Å)	0.71073 Å
crystal system, space group	Trigonal, R-3
a (Å)	30.487(4)
b (Å)	30.487(4)
c (Å)	15.094(3)
V (Å^3)	12150(3)
Z, D_c (Mg/m^3)	6, 1.124
F(000)	4146
θ range (deg)	1.34 to 25.08°
reflns collected/unique	26385/4804
R_{int}	0.0339
data/restraints/params	4804/48/259
GOF on F^2	1.069
R_1, wR_2 (I>2σ(I))	R_1 = 0.0413, wR_2 = 0.1226
R_1, wR_2 (all data)	R_1 = 0.0478, wR_2 = 0.1279

Table S2. Selected bond lengths [Å] and angles [º] for **JLU-Liu45**.

JLU-Liu45			
Zr(1)-O(5')#1	1.959(6)	C(3)-C(4)	1.400(7)
Zr(1)-O(5')	2.097(5)	C(3)-C(14)	1.475(6)
Zr(1)-O(5')#2	2.098(5)	C(5)-C(6)	1.386(6)
Zr(1)-O(6)	2.1341(16)	C(7)-C(12)	1.380(6)
Zr(1)-O(2)#1	2.235(2)	C(17)-C(18)	1.369(5)
Zr(1)-O(5)	2.237(5)	C(17)-C(20)	1.502(5)
C(1)-C(6)	1.381(7)	C(5)-C(4)-C(3)	120.9(4)
C(1)-C(2)	1.389(6)	C(4)-C(3)-C(14)	120.1(4)
O(5')-Zr(1)-O(6)	1.931(4)	C(4)-C(5)-C(6)	120.4(5)
O(5')-Zr(1)#7	2.098(5)	C(12)-C(7)-C(8)	116.9(12)
O(1)-Zr(1)-O(5)#2	142.21(16)	O(4)-C(20)-O(3)	127.3(3)
O(5')#1-Zr(1)-O(3)#3	141.73(16)	O(4)-C(20)-C(17)	116.4(3)
O(5')-Zr(1)-O(3)#3	143.00(17)	O(3)-C(20)-C(17)	116.3(3)
O(5')#2-Zr(1)-O(3)#3	86.01(17)	O(1)-C(13)-O(2)	127.0(3)
O(6)-Zr(1)-O(3)#3	77.22(12)	O(1)-C(13)-C(10)	116.4(3)
O(1)-Zr(1)-O(3)#3	120.78(9)	C(8)-C(7)-C(8')	22.0(14)

Symmetry transformations used to generate equivalent atoms:

#1 y,-x+y,-z #2 -x+y,-x,z #3 x-y+1/3,x-1/3,-z+2/3 #4 -x+1/3,-y+2/3,-z+2/3 #5 x-y,x,-z #6 y+1/3,-x+y+2/3,-z+2/3

Table S3 Force fields parameters of the GCMC simulations.

Atom	σ (Å)	ε/k_B (K)
Zr	2.783	34.691
C	3.473	47.813
O	3.033	48.115
H	2.846	7.642

Table S4 Atomic partial charges of JLU-Liu45 for the GCMC simulations.

JLU-Liu45							
Zr1	0.4989	C61	-0.0518	C121	-0.0169	C181	-0.0596
O2	-0.1974	H62	0.04	C122	-0.0626	H182	0.0325
O3	-0.1984	C63	-0.0672	H123	0.0373	C183	-0.0457
O4	-0.1995	H64	0.0372	C124	-0.0121	H184	0.0394
O5	-0.198	C65	0.1801	C125	-0.0504	C185	-0.0183
O6	-0.3316	C66	-0.0168	H126	0.0459	C186	-0.0487
C7	-0.0169	C67	-0.0596	C127	-0.0484	H187	0.0432
C8	-0.0626	H68	0.0325	H128	0.0551	C188	-0.0618
H9	0.0373	C69	-0.0457	C129	-0.0631	H189	0.0385
C10	-0.0121	H70	0.0394	H130	0.0406	C190	0.1837
C11	-0.0504	C71	-0.0183	C131	-0.0201	Z191	0.4989
H12	0.0459	C72	-0.0487	C132	-0.0658	O192	-0.1973
C13	-0.0484	H73	0.0432	H133	0.036	O193	-0.1985
H14	0.0551	C74	-0.0618	C134	-0.0502	O194	-0.1995
C15	-0.0631	H75	0.0385	H135	0.0417	O195	-0.198
H16	0.0406	C76	0.1837	C136	-0.0215	O196	-0.3317
C17	-0.0201	Z77	0.4989	C137	-0.0517	C197	-0.0169
C18	-0.0658	O78	-0.1973	H138	0.0401	C198	-0.0625
H19	0.036	O79	-0.1985	C139	-0.0672	H199	0.0373
C20	-0.0502	O80	-0.1995	H140	0.0372	C200	-0.012
H21	0.0417	O81	-0.198	C141	0.1801	C201	-0.0504
C22	-0.0215	O82	-0.3317	C142	-0.0167	H202	0.0459
C23	-0.0517	C83	-0.0169	C143	-0.0595	C203	-0.0483
H24	0.0401	C84	-0.0625	H144	0.0325	H204	0.0552
C25	-0.0672	H85	0.0373	C145	-0.0455	C205	-0.0631
H26	0.0372	C86	-0.012	H146	0.0393	H206	0.0406
C27	0.1801	C87	-0.0504	C147	-0.0182	C207	-0.02
C28	-0.0167	H88	0.0459	C148	-0.0486	C208	-0.0657
C29	-0.0595	C89	-0.0483	H149	0.0432	H209	0.0361
H30	0.0325	H90	0.0552	C150	-0.0617	C210	-0.0501
C31	-0.0455	C91	-0.0631	H151	0.0385	H211	0.0418
H32	0.0393	H92	0.0406	C152	0.1838	C212	-0.0214
C33	-0.0182	C93	-0.02	Z153	0.4991	C213	-0.0517
C34	-0.0486	C94	-0.0657	O154	-0.1973	H214	0.0401
H35	0.0432	H95	0.0361	O155	-0.1984	C215	-0.0671

C36	-0.0617	C96	-0.0501	O156	-0.1994	H216	0.0372
H37	0.0385	H97	0.0418	O157	-0.1981	C217	0.1801
C38	0.1838	C98	-0.0214	O158	-0.3317	C218	-0.0167
Z39	0.4991	C99	-0.0517	C159	-0.0169	C219	-0.0594
O40	-0.1973	H100	0.0401	C160	-0.0626	H220	0.0324
O41	-0.1984	C101	-0.0671	H161	0.0373	C221	-0.0456
O42	-0.1994	H102	0.0372	C162	-0.0121	H222	0.0393
O43	-0.1981	C103	0.1801	C163	-0.0504	C223	-0.0182
O44	-0.3317	C104	-0.0167	H164	0.0459	C224	-0.0485
C45	-0.0169	C105	-0.0594	C165	-0.0484	H225	0.0431
C46	-0.0626	H106	0.0324	H166	0.0551	C226	-0.0617
H47	0.0373	C107	-0.0456	C167	-0.0632	H227	0.0385
C48	-0.0121	H108	0.0393	H168	0.0406	C228	0.1837
C49	-0.0504	C109	-0.0182	C169	-0.0201	O229	-0.3337
H50	0.0459	C110	-0.0485	C170	-0.0659	O230	-0.3337
C51	-0.0484	H111	0.0431	H171	0.036		
H52	0.0551	C112	-0.0617	C172	-0.0502		
C53	-0.0632	H113	0.0385	H173	0.0417		
H54	0.0406	C114	0.1837	C174	-0.0215		
C55	-0.0201	Z115	0.4989	C175	-0.0518		
C56	-0.0659	O116	-0.1974	H176	0.04		
H57	0.036	O117	-0.1984	C177	-0.0672		
C58	-0.0502	O118	-0.1995	H178	0.0372		
H59	0.0417	O119	-0.198	C179	0.1801		
C60	-0.0215	O120	-0.3316	C180	-0.0168		

Table S5 A comparison of chemical stability of JLU-Liu45 with other stable Zr-MOFs materials.

Compound	pH values	Reference
JLU-Liu45	0-11	This work
PCN-223	0-10	1
PCN-777	3-11	2
PCN-56	2-11	3
PCN-59	2-11	3
PCN-225	0-12	4
BUT-12	0-10	5
BUT-13	0-10	5
BUT-14	0-10	6
BUT-15	0-10	6
NPF-200	1-12	7
PCN-134	0-13	8

Table S6. CO_2 adsorption capacities and Q_{st} values in reported Zr-MOFs at 273 K and 1 bar.

Zr-MOFs	BET surface area ($m^2\ g^{-1}$)	CO_2 uptake (273 K, $cm^3\ g^{-1}$)	CO_2 uptake (298 K)	Q_{st} values ($kJ\ mol^{-1}$)	Ref.
JLU-Liu45	**971**	**116**	**66**	**34**	**This work**
BUT-10	1310	92	53.5	22	9
BUT-11	1848	89	50.6	26	9
UiO-67	2505	N.A.	22.9	16	9
493-MOF-TATB	820	97	60	25	10
493-MOF-BA	1265	78	50	23	10
493-MOF-NA	1199	85	56	20	10
LIFM-28np	940	29.0	N.A.	22	11
LIFM-79	1689	76.3	~42	32	11
LIFM-77	1619	81.0	~44	34	11
PCN-56	3741	~58	~37[a]	20	3
PCN-57	2572	~50	~33[a]	22	3
PCN-58	2185	~63	~40[a]	24	3
PCN-59	1279	~71	~42[a]	32	3
NU-1000	2320	N.A.	~40[b]	17	12
SALI-9	870	N.A.	~18[b]	34	12
SALI-1’	1600	N.A.	~34[b]	21	12
CPM-99(H_2)	N.A.	73	~50	N.A.	13
CPM-99(Zn)	N.A.	60	~35	N.A.	13
CPM-99(Co)	N.A.	61	~42	N.A.	13
CPM-99(Fe)	1030	76	~45	N.A.	13
MOF-892	1431	~41	~22	24	14
MOF-893	558	~40	~21	31	14
JLU-MOF50	1101	69	35	25	15
JLU-MOF58	3663	49	28	19	16
Corrole-MOF-1	2545	76	46	N.A.	17
PCN-138	1261	63	41	N.A.	18
MIP-203-F	430	61	46	32	19
MIP-203-S	no	36	15	34	19
MIP-203-M	380	48	36	33	19

[a]at 296 K, [b]at 293 K.

Table S7. Gas adsorption data for **JLU-Liu45**.

Compound	N_2[a]		CO_2[a]			CH_4[a]	
	77 K	298 K	195 K	273 K	298 K	273 K	298 K
JLU-Liu45	256	3	216	116	66	27	16
Compound	C_2H_6[a]		C_3H_8[a]			H_2O	
	273 K	298 K	273 K	298 K		298 K	
JLU-Liu45	85	65	74	63		0.16 mg/mg	

[a] Gas uptake in $cm^3\ g^{-1}$.

Table S8. Comparison of CO_2/N_2 (0.15/0.85) selectivity of **JLU-Liu45** with other stable MOFs.

Zr-MOFs	CO_2/N_2 selectivity	Ref.
JLU-Liu45	**81.4**	**This work**
MIL-101	12.6	20
MIL-125-NH_2	27.0	21
MIL-68-Al	37.0	22
ZIF-68	18.0	23
ZIF-69	20.0	23
ZIF-70	17.0	23
ZIF-79	23.0	23
ZIF-81	24.0	23
ZIF-95	18.0	24
UiO-66(Br)	25.1	25
UiO-66(NO_2)	26.4	25
UiO-66	13.4	25
UiO-67	9.4	9
BUT-10	18.6	9
BUT-11	31.5	9
BUT-11(AcOH)	24.1	26
LIFM-77	34.7	11
LIFM-79	25.2	11
LIFM-28np	5.5	11
MIP-203-F	15	19
MIP-203-S	34	19
MIP-203-M	51	19
UiO-66(Zr)-$(OH)_2$	66	27
UiO-66(Zr)-$(OAc)_2$	42.5	27
UiO-66(Zr)-(OPr)2	39.1	27
Opt-UiO-66(Zr)-$(OH)_2$	44.5	28
UiO-66-NH_2	32.3	29
UiO-66(Zr)-$(COOH)_2$	35.4	30
75PEI@meso-UiO-66-0.2Cu	59.4	31
UiO-66(Zr)-$(COOK)_2$	69.3	32
UiO-66(Zr)-$(COONa)_2$	58.0	32

Table S9. Comparison of CO_2/CH_4 (0.5/0.5) selectivity of **JLU-Liu45** with other MOFs materials.

MOFs material	CO_2/CH_4 selectivity	Ref.
JLU-Liu45	7.0	This work
MOF-177	0.9	33
ZIF-8	1.4	33
$Cu_3(BTC)_2$	2.3	33
NOTT-125	4.8	34
FJI-C1	5.9	35
ZJNU-59	6.0	36
NOTT-122	6.4	37
ZJNU-40	6.6	38
ZJNU-69	7.1	39
BSF-1	7.5	40
MFM-126	11.7	41
SNIFSIX-1-Cu	12.1	42

Table S10. Comparison of detection ability of **JLU-Liu45** towards TNP in the water with other materials.

Material	Quenching constant (K_{SV}) for TNP	Ref.
JLU-Liu45	**2.3×10^5 M^{-1}**	**This work**
UiO-67@N	2.9×10^4 M^{-1}	43
$[Eu_3(L)_3(HCOO)(\mu_3\text{-}OH)_2(H_2O)]\cdot x(solv)$	2.1×10^4 M^{-1}	44
UiO-68@NH_2	5.8×10^4 M^{-1}	45
BUT-12	3.1×10^5 M^{-1}	5
BUT-13	5.1×10^5 M^{-1}	5
$[Cd(NDC)L]_2\cdot H_2O$	3.7×10^4 M^{-1}	46
$[Zn_4(DMF)(Ur)_2(NDC)_4]$	10.8×10^4 M^{-1}	47
$[Zn_8(ad)_4(BPDC)_6O\cdot2Me_2NH_2]\cdot G$	4.6×10^4 M^{-1}	48
$[Zn(NDC)(H_2O)]n$	6×10^4 M^{-1}	49
$[Cd(NDC)_{0.5}(PCA)]\cdot xG$	3.5×10^4 M^{-1}	50
In-ADBA	1.3×10^5 M^{-1}	51
$[Tb_2(H_2L)_3(H_2O)_2]\cdot21H_2O$	1.5×10^4 M^{-1}	52
$[Cd_2(tdz)_2(4,4'\text{-}bpy)_2]\cdot6.5H_2O$	4.9×10^4 M^{-1}	53
TFPC-NDA-COF	2.5×10^5 M^{-1}	54

10. REFERENCES

1. D. Feng, Z. Y. Gu, Y. P. Chen, J. Park, Z. Wei, Y. Sun, M. Bosch, S. Yuan and H. C. Zhou, *J. Am. Chem. Soc.*, 2014, **136**, 17714-17717.
2. D. Feng, K. Wang, J. Su, T. F. Liu, J. Park, Z. Wei, M. Bosch, A. Yakovenko, X. Zou and H. C. Zhou, *Angew. Chem. Int. Ed.*, 2015, **54**, 149-154.
3. H. L. Jiang, D. Feng, T. F. Liu, J. R. Li and H. C. Zhou, *J. Am. Chem. Soc.*, 2012, **134**, 14690-14693.
4. H. L. Jiang, D. Feng, K. Wang, Z. Y. Gu, Z. Wei, Y. P. Chen and H. C. Zhou, *J. Am. Chem. Soc.*, 2013, **135**, 13934-13938.
5. B. Wang, X. L. Lv, D. Feng, L. H. Xie, J. Zhang, M. Li, Y. Xie, J. R. Li and H. C. Zhou, *J. Am.*

Chem. Soc., 2016, **138**, 6204-6216.

6. B. Wang, Q. Yang, C. Guo, Y. Sun, L. H. Xie and J. R. Li, *ACS Appl. Mater. Interfaces*, 2017, **9**, 10286-10295.

7. X. Zhang, X. Zhang, J. A. Johnson, Y. S. Chen and J. Zhang, *J. Am. Chem. Soc.*, 2016, **138**, 8380-8383.

8. S. Yuan, J. S. Qin, L. Zou, Y. P. Chen, X. Wang, Q. Zhang and H. C. Zhou, *J. Am. Chem. Soc.*, 2016, **138**, 6636-6642.

9. B. Wang, H. Huang, X. L. Lv, Y. Xie, M. Li and J. R. Li, *Inorg. Chem.*, 2014, **53**, 9254-9259.

10. C. S. Liu, Z. H. Zhang, M. Chen, H. Zhao, F. H. Duan, D.-M. Chen, M. H. Wang, S. Zhang and M. Du, *Chem. Commun.*, 2017, **53**, 3941-3944.

11. C. X. Chen, Z. W. Wei, J. J. Jiang, S. P. Zheng, H. P. Wang, Q. F. Qiu, C. C. Cao, D. Fenske and C. Y. Su, *J. Am. Chem. Soc.*, 2017, **139**, 6034-6037.

12. P. Deria, J. E. Mondloch, E. Tylianakis, P. Ghosh, W. Bury, R. Q. Snurr, J. T. Hupp and O. K. Farha, *J. Am. Chem. Soc.*, 2013, **135**, 16801-16804.

13. Q. Lin, X. Bu, A. Kong, C. Mao, X. Zhao, F. Bu and P. Feng, *J. Am. Chem. Soc.*, 2015, **137**, 2235-2238.

14. P. T. K. Nguyen, H. T. D. Nguyen, H. N. Nguyen, C. A. Trickett, Q. T. Ton, E. Gutiérrez-Puebla, M. A. Monge, K. E. Cordova and F. Gándara, *ACS Appl. Mater. Interfaces*, 2018, **10**, 733-744.

15. X. Sun, S. Yao, C. Yu, G. Li, C. Liu, Q. Huo and Y. Liu, *J. Mater. Chem.A*, 2018, **6**, 6363-6369.

16. X. Sun, J. Gu, Y. Yuan, C. Yu, J. Li, H. Shan, G. Li and Y. Liu, *Inorg. Chem.*, 2019, **58**, 7480-7487.

17. Y. Zhao, S. Qi, Z. Niu, Y. Peng, C. Shan, G. Verma, L. Wojtas, Z. Zhang, B. Zhang, Y. Feng, Y.-S. Chen and S. Ma, *J. Am. Chem. Soc.*, 2019, **141**, 14443-14450.

18. Y.-C. Qiu, S. Yuan, X.-X. Li, D.-Y. Du, C. Wang, J.-S. Qin, H. F. Drake, Y.-Q. Lan, L. Jiang and H.-C. Zhou, *J. Am. Chem. Soc.*, 2019, **141**, 13841-13848.

19. S. Wang, N. Xhaferaj, M. Wahiduzzaman, K. Oyekan, X. Li, K. Wei, B. Zheng, A. Tissot, J. Marrot, W. Shepard, C. Martineau-Corcos, Y. Filinchuk, K. Tan, G. Maurin and C. Serre, *J. Am. Chem. Soc.*, 2019, **141**, 17207-17216.

20. K. Munusamy, G. Sethia, D. V. Patil, P. B. Somayajulu Rallapalli, R. S. Somani and H. C. Bajaj, *Chem. Eng. J.*, 2012, **195-196**, 359-368.

21. S. N. Kim, J. Kim, H. Y. Kim, H. Y. Cho and W. S. Ahn, *Catal. Today*, 2013, **204**, 85-93.

22. Q. Yang, S. Vaesen, M. Vishnuvarthan, F. Ragon, C. Serre, A. Vimont, M. Daturi, G. De Weireld and G. Maurin, *J. Mater. Chem.*, 2012, **22**, 10210-10220.

23. R. Banerjee, H. Furukawa, D. Britt, C. Knobler, M. O'Keeffe and O. M. Yaghi, *J. Am. Chem. Soc.*, 2009, **131**, 3875-3877.

24. B. Wang, A. P. Côté, H. Furukawa, M. O'Keeffe and O. M. Yaghi, *Nature*, 2008, **453**, 207.

25. W. Zhang, H. Huang, C. Zhong and D. Liu, *PCCP*, 2012, **14**, 2317-2325.

26. P. Xydias, I. Spanopoulos, E. Klontzas, G. E. Froudakis and P. N. Trikalitis, *Inorg. Chem.*, 2014, **53**, 679-681.

27. Y. Wang, Z. Hu, T. Kundu, Y. Cheng, J. Dong, Y. Qian, L. Zhai and D. Zhao, *ACS Sustainable Chem. Eng.*, 2018, 6, 11904-11912.

28. Z. Hu, Y. Wang, S. Farooq and D. Zhao, *AlChE J.*, 2017, 63, 4103-4114.

29. G. E. Cmarik, M. Kim, S. M. Cohen and K. S. Walton, *Langmuir*, 2012, 28, 15606-15613.

30. Z. Hu, Y. Peng, Z. Kang, Y. Qian and D. Zhao, *Inorg. Chem.*, 2015, 54, 4862-4868.

31. Z. Li, H. Chen, C. Chen, Q. Guo, X. Li, Y. He, H. Wang, N. Feng, H. Wan and G. Guan, *Chem. Eng. J.*, 2019, 375, 121962.
32. Z. Hu, M. Khurana, Y. H. Seah, M. Zhang, Z. Guo and D. Zhao, *Chem. Eng. Sci.*, 2015, 124, 61-69.
33. Z. Xiang, X. Peng, X. Cheng, X. Li and D. Cao, *J. Phys. Chem. C*, 2011, 115, 19864-19871.
34. N. H. Alsmail, M. Suyetin, Y. Yan, R. Cabot, C. P. Krap, J. Lü, T. L. Easun, E. Bichoutskaia, W. Lewis, A. J. Blake and M. Schröder, *Chem. Eur. J.*, 2014, 20, 7317-7324.
35. Y. Huang, Z. Lin, H. Fu, F. Wang, M. Shen, X. Wang and R. Cao, *ChemSusChem*, 2014, 7, 2647-2653.
36. Y. Wang, M. He, X. Gao, S. Li, S. Xiong, R. Krishna and Y. He, *ACS Appl. Mater. Interfaces.*, 2018, 10, 20559-20568.
37. Y. Yan, M. Suyetin, E. Bichoutskaia, A. J. Blake, D. R. Allan, S. A. Barnett and M. Schröder, *Chem. Sci.*, 2013, 4, 1731-1736.
38. C. Song, Y. He, B. Li, Y. Ling, H. Wang, Y. Feng, R. Krishna and B. Chen, *Chem. Commun.*, 2014, 50, 12105-12108.
39. F. Chen, Y. Wang, D. Bai, M. He, X. Gao and Y. He, *J. Mater. Chem. A.*, 2018, 6, 3471-3478.
40. Y. Zhang, L. Yang, L. Wang, S. Duttwyler and H. Xing, *Angew. Chem. Int. Ed.*, 2019, 58, 8145-8150.
41. J. D. Humby, O. Benson, G. L. Smith, S. P. Argent, I. da Silva, Y. Cheng, S. Rudić, P. Manuel, M. D. Frogley, G. Cinque, L. K. Saunders, I. J. Vitórica-Yrezábal, G. F. S. Whitehead, T. L. Easun, W. Lewis, A. J. Blake, A. J. Ramirez-Cuesta, S. Yang and M. Schröder, *Chem. Sci.*, 2019, 10, 1098-1106.
42. P. Nugent, V. Rhodus, T. Pham, B. Tudor, K. Forrest, L. Wojtas, B. Space and M. Zaworotko, *Chem. Commun.*, 2013, 49, 1606-1608.
43. S. S. Nagarkar, A. V. Desai and S. K. Ghosh, *Chem. Commun.*, 2014, **50**, 8915-8918.
44. X.-Z. Song, S.-Y. Song, S.-N. Zhao, Z.-M. Hao, M. Zhu, X. Meng, L. L. Wu and H. J. Zhang, *Adv. Funct. Mater.*, 2014, **24**, 4034-4041.
45. S. S. Nagarkar, A. V. Desai, P. Samanta and S. K. Ghosh, *Dalton Trans.*, 2015, **44**, 15175-15180.
23. B. Wang, X. L. Lv, D. Feng, L. H. Xie, J. Zhang, M. Li, Y. Xie, J. R. Li and H. C. Zhou, *J. Am. Chem. Soc.*, 2016, **138**, 6204-6216.
46. B. Q. Song, C. Qin, Y. T. Zhang, X. S. Wu, L. Yang, K. Z. Shao and Z. M. Su, *Dalton Trans.*, 2015, **44**, 18386-18394.
47. S. Mukherjee, A. V. Desai, B. Manna, A. I. Inamdar and S. K. Ghosh, *Cryst. Growth Des.* 2015, **15**, 4627-4634.
48. B. Joarder, V. Desai Aamod, P. Samanta, S. Mukherjee and K. Ghosh Sujit, *Chem. Eur. J.*, 2015, **21**, 965-969.
49. P. Ghosh, K. Saha Sourav, A. Roychowdhury and P. Banerjee, *Eur. J. Inorg. Chem.*, 2015, **17**, 2851-2857.
50. S. Nagarkar Sanjog, B. Joarder, K. Chaudhari Abhijeet, S. Mukherjee and K. Ghosh Sujit, *Angew. Chem. Int. Ed.*, 2013, **125**, 2953-2957.
51. X. Liu, B. Liu, G. Li and Y. Liu, *J. Mater. Chem.A*, 2018, **6**, 17177-17185.
52. R. Fu, S. Hu and X. Wu, *J. Mater. Chem. A*, 2017, **5**, 1952-1956.
53. A. Gogia and S. K. Mandal, *Dalton Trans.* 2019, **48**, 2388-2398.
54. P. Das and S. K. Mandal, *J. Mater. Chem.A*, 2018, **6**, 16246-16256.